Reduction of the spin-torque critical current by partially canceling the free layer demagnetization field

Luqiao Liu,[a] Takahiro Moriyama, D. C. Ralph, and R. A. Buhrman
Cornell University, Ithaca, New York 14853, USA

(Received 11 February 2009; accepted 6 March 2009; published online 26 March 2009)

We significantly reduce the critical current I_{c0} for the onset of spin torque switching of the free layer in nanometer-scale in-plane magnetized spin valves by partially cancelling its intrinsic demagnetization field through the utilization of Co/Ni multilayer free layers. The out-of-plane magnetic anisotropy arising from the Co/Ni interfaces reduces the effective demagnetization field (H_{eff}) while not significantly affecting the thermal stability of the free layer. A zero-thermal-fluctuation critical current density $J_{c0} \sim 2 \times 10^6$ A/cm^2 is determined through both current ramp rate and nanosecond pulse measurements, and comparisons with large H_{eff} control samples confirm that this strategy is efficient in substantially decreasing I_{c0}. © *2009 American Institute of Physics*. [DOI: 10.1063/1.3107262]

Spin torque (ST) induced magnetic moment reversal has been intensively studied, since its theoretical prediction[1,2] and experimental confirmation,[3,4] in large part because the ability of spin-polarized currents to switch the orientation of a nanomagnet rapidly and reversibly could find broad application in magnetic random access memory (MRAM).[5–7] For the successful realization of ST-MRAM, a low critical current (I_c) for ST reversal is crucial, both for compatibility with highly scaled complementary metal-oxide-semiconductor technology and for low power consumption. For conventional in-plane magnetized nanomagnets in zero magnetic field, I_c is expected to have the form (in the macrospin limit)[4,8]

$$I_c \approx \frac{2e}{\hbar}\frac{\alpha M_S V}{g(\theta)P}\left(H_c + \frac{H_{\text{eff}}}{2}\right), \tag{1}$$

where α is the Gilbert damping, M_S is the saturation magnetization of the switching layer, V is its volume, P is the spin current polarization, $g(\theta)$ is a ST efficiency, H_c is the in-plane coercive field, and H_{eff} is the effective out-of-plane demagnetization field. Since H_{eff} is usually of the order of 1 T, much greater than H_c, ordinarily it is the large value of H_{eff} that restricts efforts to reduce I_c. In contrast, the nanomagnet's thermal stability is determined by H_c, independent of H_{eff}.[7] One strategy that has been attempted for reducing I_c while maintaining thermal stability is to utilize magnetic materials with perpendicular magnetic anisotropy (PMA), with a sufficiently large out-of-plane anisotropy field $H_{K\perp}$ that in equilibrium the magnetization points out of plane.[9–13] I_c then has the same field dependence as the energy barrier for thermal stability. However, to date, no significant reduction in I_c has been demonstrated experimentally with PMA ST devices in comparison to the I_c of in-plane magnetized devices. This is likely due to either a low spin polarization[9,14] or a large damping[13] in the PMA materials that have been employed. Another disadvantage associated with the PMA approach is that a perpendicularly oriented fixed magnetic layer exerts a large dipole field on the free (switching) layer,[9,14] an effect that can be eliminated for the in-plane magnetized case with the use of properly balanced synthetic antiferromagnetic fixed layers.

In this work, we reduce I_c by combining the magnetic advantages of in-plane magnetized samples with capability of PMA structures to tune the demagnetization field. Rather than employing a material with a very large $H_{K\perp}$ that dominates the intrinsic demagnetization field H_d of the free layer to give PMA, we only partially cancel H_d with a moderate $H_{K\perp}$. When both the demagnetization field and an out-of-plane crystalline (interface) anisotropy field are present, the combined anisotropy energy of a thin-film nanomagnet is

$$\begin{aligned} E_{\text{tot}} &= E_{K\perp} + E_{\text{demag}} = \tfrac{1}{2}H_{K\perp}M_S \cos^2\theta + \tfrac{1}{2}H_d M_S \sin^2\theta \\ &= \tfrac{1}{2}(H_d - H_{K\perp})M_S \sin^2\theta + \text{const.}, \end{aligned} \tag{2}$$

where θ is the angle between the magnetic moment and the film plane. The combined anisotropy is still uniaxial (within this first order approximation for $E_{K\perp}$), so that in equilibrium the magnetic moment will be either in the film plane (when $H_d > H_{K\perp}$) or perpendicular to the plane (when $H_d < H_{K\perp}$). We show that by reducing the total effective anisotropy $H_{\text{eff}} = H_d - H_{K\perp}$ well below H_d, while keeping $H_{\text{eff}} > 0$, I_c can be reduced by a factor of 5–6. The fact that the equilibrium magnetic moment still lies in plane provides great freedom in the choice of the fixed layer materials and structures, making our approach highly flexible.

In our experiment, Co/Ni multilayers were deposited using a dc sputtering system with a base pressure less than 5×10^{-9} torr. We employed Co/Ni multilayers because $H_{K\perp}$ in this system can be tuned over a wide range by changing the thickness of each layer and/or the number of repeats.[15] A $[\text{Ta}(5)/\text{CuN}_x(20)]_3/\text{Ta}(5)/\text{Cu}(3)$ (thickness in nanometers) seeding layer was used to provide a smooth base layer with [111] texture, as verified by x-ray diffraction. By testing Co/Ni multilayers with different thicknesses and repeats, we determined that a $[\text{Co}(0.4)/\text{Ni}(1)]_2/\text{Co}(0.4)$ multilayer would achieve the desired condition that $0 < H_{\text{eff}} \ll H_d$. Perpendicular-to-plane M-H curves, as measured by a vibrating sample magnetometer, of continuous film samples of this low demagnetization field (LD) material are as shown in Fig. 1(a). For comparison, we also made a control sample composed of Ni(2)/Co(1.2) whose high demagnetization field

[a]Electronic mail: ll293@cornell.edu.

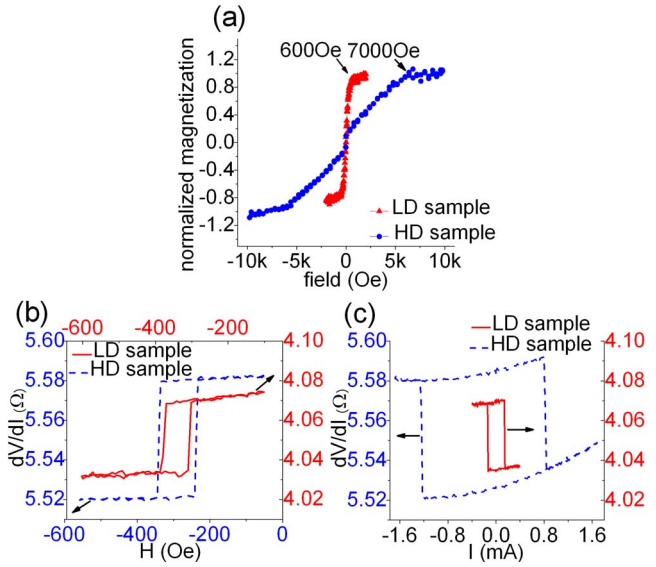

FIG. 1. (Color online) (a) *M-H* curves for Co/Ni based continuous films measured with the magnetic field applied perpendicular to the film plane. The red triangles correspond to a $[Co(0.4)/Ni(1)]_2/Co(0.4)$ (units in nanometers) film, while the blue circles represent a Ni(2)/Co(1.2) thin film. (b) Magnetoresistance minor loop for the LD sample (red solid) and HD sample (blue dash), respectively. (c) Spin transfer loop for the LD sample (red solid) and HD sample (blue dash), respectively. All of the data are taken at room temperature.

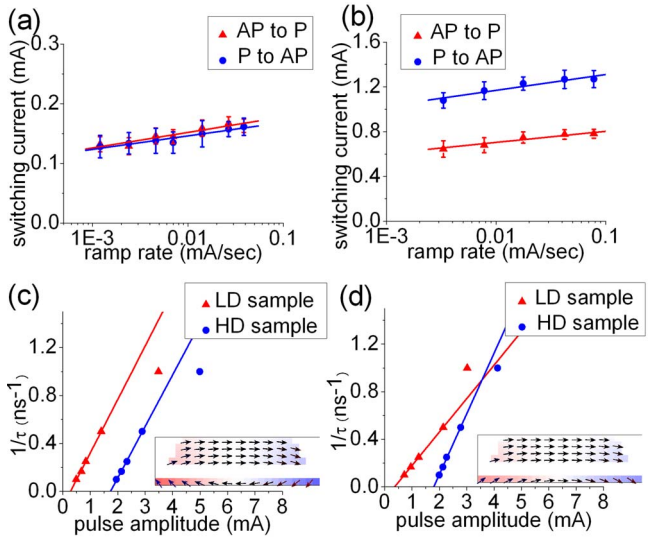

FIG. 2. (Color online) Switching currents as a function of the ramp rate for (a) the LD sample and (b) the HD sample. The red triangles denote AP to P switching and the blue circles P to AP switching. (c) and (d), The inverse of pulse width as a function of the average pulse amplitude required for (c) AP to P and (d) P to AP switching, with the red triangles for LD sample and the blue circles for HD sample. Insets: Micromagnetic simulations for the LD sample in (c) the AP configuration and (d) the P configuration showing that the magnetizations in both the free and fixed layers are canted significantly out of plane.

(HD) *M-H* response is also shown in Fig. 1(a). The demagnetization field of the LD sample is reduced from ~7000 to ~600 Oe due to the presence of the perpendicular anisotropy arising from the multiple Co/Ni interfaces. The in-plane *M-H* curve for the LD sample shows that the in-plane remnant magnetization is $\sim 0.9M_S$, indicating a good easy-plane anisotropy.

With the free layer composition determined we then produced multilayer stacks with the composition: seeding layer/free layer/Cu(8 nm)/Permalloy(20 nm)/capping layer. We patterned the stacks into elliptical nanopillars with the cross section area $\sim 90 \times 190$ nm^2 using e-beam lithography and ion-beam etching. We also made HD control samples with the same device size and stack composition, except that the free layer was replaced with the simple Ni(2)/Co(1.2) structure. At least three devices of each type were measured, and similar results were obtained for all devices of each type. In the following we present data from one device of each type.

The field-in-plane minor magnetoresistance loop of a LD device, taken at room temperature, is shown in Fig. 1(b). Its coercive field H_c is ~43 Oe and the magnetoresistance ΔR is ~40 mΩ. A current scan showing ST-induced switching, taken with the dipole field from the permalloy fixed layer cancelled by an applied field, is plotted in Fig. 1(c). The quasistatic switching currents were ~0.14 mA for both the antiparallel to parallel (AP-P) switching and the parallel to antiparallel (P-AP) switching. For comparison, the corresponding minor loop and spin transfer loop for the HD sample are plotted as the blue curves in Figs. 1(b) and 1(c). For the HD sample, $H_c \sim 52$ Oe and $\Delta R \sim 60$ mΩ, and the switching currents were $I_{\text{AP-P}}=0.81$ mA and $I_{\text{P-AP}}=-1.24$ mA. We note that ΔR for the HD sample is about 1.5 times larger than that for the LD sample. We believe that this difference is due to different spin polarization values in the Co/Ni films. Although both the LD and the HD free layers are terminated with Co, the thicknesses of the terminating Co layer are different: 0.4 nm for the LD sample and 1.2 nm for the HD sample. Previous experiments have shown that a Co thickness of order ~1 nm is needed to achieve the maximum spin filtering effect.[16]

To determine the energy barrier U against thermally activated magnetic reversal and the zero-thermal-fluctuation critical current I_{c0}, a ramp rate measurement was carried out for both the LD samples and the HD samples. The results are shown in Figs. 2(a) and 2(b). In the thermally activated switching regime, the switching current $\langle I_c \rangle$ and ramp rate $\dot{I}$ are related as[17,18]

$$\langle I_c \rangle = I_{c0}\left[1 - \frac{k_B T}{U}\ln\left(\frac{k_B T}{U}\frac{I_{c0}/\tau_0}{\dot{I}}\right)\right], \tag{3}$$

where T is the temperature and τ_0 is an attempt rate, assumed to be 1 ns. For each point, we obtained $\langle I_c \rangle$ by averaging over 25 scans. For the LD sample by fitting to Eq. (3) we obtained $U_{\text{AP-P}}=0.88$ eV, $U_{\text{P-AP}}=0.92$ eV, $I_{c0,\text{AP-P}}=0.39$ mA, and $I_{c0,\text{P-AP}}=-0.35$ mA. The corresponding parameters for the HD sample were $U_{\text{AP-P}}=1.00$ eV, $U_{\text{P-AP}}=1.08$ eV, $I_{c0,\text{AP-P}}=1.66$ mA, and $I_{c0,\text{P-AP}}=-2.54$ mA. Therefore, the critical currents for the LD sample are reduced by a factor of ~5 for both directions compared to the HD sample, while the thermal stability is compromised by less than 20%. The decrease in the critical currents (~5×) agrees reasonably well with the reduction in H_{eff}(~11×) after taking into account the change in spin polarization (~1.5×) and the fact that for $H_{\text{eff}} \sim 600$ Oe, the relationship $H_{\text{eff}}/2 \gg H_c$ does not hold precisely in Eq. (1). (Note H_c here should be the non-thermal fluctuation value). The small change in thermal stability is in good agreement with expectations based on the H_c values of the LD and HD samples.

A practical ST-MRAM element must undergo switching on the nanosecond timescale, so we performed pulse measurements with pulse width varying from 1 to 10 ns to study this regime. The results are summarized in Figs. 2(c) and 2(d). According to spin transfer theory within the macrospin approximation, for $I > I_{c0}$ a linear relationship should exist between the switching speed τ^{-1} and the amplitude of the applied current pulse,[8]

$$\tau^{-1} = \frac{Pg(\theta)(\mu_B/e)}{M_S V \ln(\pi/2\theta_0)}(I - I_{c0}), \tag{4}$$

where θ_0 is the initial angle between the free layer and the fixed layer. For very large amplitude and short ($\tau = 1$ ns) pulses we observe a deviation from a linear dependence on I for both types of samples, similar to previous results,[19,20] and so we did not include the 1 ns points in the linear fits. This deviation is perhaps due to nonuniform effects in the high speed reversal. The values of I_{c0} determined from the fits are, for the LD sample $I_{c0,\text{AP-P}} = 0.28$ mA and $I_{c0,\text{P-AP}} = -0.36$ mA, and for the HD sample $I_{c0,\text{AP-P}} = 1.74$ mA and $I_{c0,\text{P-AP}} = -1.79$ mA. These values agree reasonably well with the numbers obtained from the ramp rate measurements discussed above, given the possibility of differences between the reversal processes in the two cases. The slopes $\zeta \equiv d(\tau^{-1})/dI$ of the ST switching curves in the linear regime should [according to Eq. (4)] be determined by the spin polarization P and the initial angle θ_0, for a given value of the magnetic moment for the free layer. Since P_{HD} is about 1.5 times larger than P_{LD}, one might expect that the slopes should scale the same way. However for AP to P switching, we find $\zeta_{\text{HD}}/\zeta_{\text{LD}} \approx 1$, while $\zeta_{\text{HD}}/\zeta_{\text{LD}} \approx 1.8$ for P to AP switching. This difference can be qualitatively explained by micromagnetic simulations for the two cases.[21] In both the LD and HD samples, the Py fixed layer is expected to cant near its edges due to the tapered sidewalls of the sample, thereby producing a nonuniform dipole field acting on the free layer.[20] As is shown in the insets of Figs. 2(c) and 2(d), for the LD device the low value of H_{eff} allows the edges of the free layer magnetization to curl or cant significantly out of plane in response to this dipole field. However, for the HD sample (not shown), due to the larger H_{eff} no significant curling is observed in simulation. For the LD sample, in the AP state the fixed layer and the free layer will curl in the opposite direction, hence resulting in a large initial angle θ_0, while for the P state the curling will be in the same direction, giving a small θ_0. This difference in θ_0 can affect the switching speed.[20] The canting in the LD sample can also account for the reduction in the coercive field and in thermal stability.

A further demonstration that the reduction of I_c is due to the decreased H_{eff} rather than other factors comes from samples with the free layer composition $[\text{Co}(0.4)/\text{Ni}(1)]_4/\text{Co}(0.4)$, with $H_{\text{eff}} \sim 1000$ Oe. Measurements on a device with this free layer yielded $I_{c0,\text{AP-P}} \approx 0.95$ mA, $I_{c0,\text{P-AP}} \approx -0.62$ mA (ramp rate method), and $I_{c0,\text{AP-P}} \approx 0.6$ mA and $I_{c0,\text{P-AP}} \approx -0.4$ mA (pulse method). Given that the total magnetic moment of this sample is roughly twice that of LD and HD samples discussed above, these critical currents are also in good agreement with Eq. (1).

In summary, we have fabricated spin valve devices with an in-plane magnetized free layer that has a low effective demagnetization field. The zero-thermal-fluctuation critical current I_{c0} is reduced by a factor of 5–6 in comparison to high H_{eff} control samples that have the same total magnetic moment, while the thermal stability is almost the same. A further reduction by a factor of 2–4 in J_c would be expected if the spin polarization could be optimized (for example, by use of a magnetic tunnel junction rather than a spin valve). If this is successfully achieved, this type of structure should allow J_c to be reduced into the 5×10^5 A/cm^2 regime, where a practical ST-MRAM technology could be implemented.

This work was supported in part by the Office of Naval Research, by the National Science Foundation (NSF)/Nanoscale Science and Engineering Center program through the Cornell Center for Nanoscale Systems, and by the Semiconductor Research Corporation. This work was performed in part at the Cornell NanoScale Facility, a member of the National Nanotechnology Infrastructure Network, which is supported by NSF Grant No. ECS 03-35765, and benefited from use of the facilities of the Cornell Center for Materials Research, which is supported by the NSF/MRSEC program.

[1] L. Berger, Phys. Rev. B **54**, 9353 (1996).
[2] J. C. Slonczewski, J. Magn. Magn. Mater. **159**, L1 (1996).
[3] E. B. Myers, D. C. Ralph, J. A. Katine, R. N. Louie, and R. A. Buhrman, Science **285**, 867 (1999).
[4] J. A. Katine, F. J. Albert, R. A. Buhrman, E. B. Myers, and D. C. Ralph, Phys. Rev. Lett. **84**, 3149 (2000).
[5] C. Chappert, A. Fert, and F. N. van Dau, Nature Mater. **6**, 813 (2007).
[6] J. A. Katine and E. E. Fullerton, J. Magn. Magn. Mater. **320**, 1217 (2008).
[7] P. M. Braganca, I. N. Krivorotov, O. Ozatay, A. G. F. Garcia, N. C. Emley, J. C. Sankey, D. C. Ralph, and R. A. Buhrman, Appl. Phys. Lett. **87**, 112507 (2005).
[8] J. Z. Sun, Phys. Rev. B **62**, 570 (2000).
[9] S. Mangin, D. Ravelosona, J. A. Katine, M. J. Carey, B. D. Terris, and E. E. Fullerton, Nature Mater. **5**, 210 (2006).
[10] D. Ravelosona, S. Mangin, Y. Lemaho, J. A. Katine, B. D. Terris, and E. E. Fullerton, Phys. Rev. Lett. **96**, 186604 (2006).
[11] H. Meng and J.-P. Wang, Appl. Phys. Lett. **88**, 172506 (2006).
[12] T. Seki, S. Mitani, and K. Takanashi, Phys. Rev. B **77**, 214414 (2008).
[13] M. Nakayama, T. Kai, N. Shimomura, M. Amano, E. Kitagawa, T. Nagase, M. Yoshikawa, T. Kishi, S. Ikegawa, and H. Yoda, J. Appl. Phys. **103**, 07A710 (2008).
[14] S. Mangin, Y. Henry, D. Ravelosona, J. A. Katine, and E. E. Fullerton, Appl. Phys. Lett. **94**, 012502 (2009).
[15] G. H. O. Daalderop, P. J. Kelly, and F. J. A. den Broeder, Phys. Rev. Lett. **68**, 682 (1992).
[16] S. K. Upadhyay, R. N. Louie, and R. A. Buhrman, Appl. Phys. Lett. **74**, 3881 (1999).
[17] F. J. Albert, N. C. Emley, E. B. Myers, D. C. Ralph, and R. A. Buhrman, Phys. Rev. Lett. **89**, 226802 (2002).
[18] J. Kurkijärvi, Phys. Rev. B **6**, 832 (1972).
[19] S. Kaka, M. R. Pufall, W. H. Rippard, T. J. Silva, S. E. Russek, J. A. Katine, and M. Carey, J. Magn. Magn. Mater. **286**, 375 (2005).
[20] P. M. Braganca, O. Ozatay, A. G. F. Garcia, O. J. Lee, D. C. Ralph, and R. A. Buhrman, Phys. Rev. B **77**, 144423 (2008).
[21] M. J. Donahue and D. G. Porter, OOMMF User's Guide, Version 1.0, National Institute of Standards and Technology Technical Report No. NISTIR 6376 1999.